LINEAR DATA ESTIMATORS FOR UW-OFDM: CLASSICAL AND BAYESIAN APPROACHES

Mario Huemer, Alexander Onic and Christian Hofbauer

Institute of Networked and Embedded Systems, Alpen-Adria-Universität Klagenfurt
Universitätsstr. 65–67, 9020, Klagenfurt, Austria
{mario.huemer, alexander.onic, chris.hofbauer}@uni-klu.ac.at
Phone: +43 463 2700-3660, Fax: +43 463 2700-3679, Web: www.nes.uni-klu.ac.at

ABSTRACT

UW-OFDM (unique word – orthogonal frequency division multiplexing) is a novel OFDM signaling concept, where the guard interval is built of a deterministic sequence – the so-called unique word – instead of the conventional random cyclic prefix. In contrast to previous attempts with deterministic sequences in the guard interval, the addressed UW-OFDM signaling approach introduces correlations between the subcarrier symbols, which can be exploited by the receiver in order to improve the bit error ratio performance. In this paper we develop several linear data estimators specifically designed for UW-OFDM, based on classical as well as on Bayesian estimation theory. We evaluate the estimators' performance for the additive white Gaussian noise channel and for selected indoor multipath channel scenarios.

1. INTRODUCTION

In [1], [2] we introduced an OFDM signaling scheme, where the usual cyclic prefixes (CP) are replaced by deterministic sequences, that we call unique words (UW). A related but – when regarded in detail – also very different scheme is KSP (known symbol padded)-OFDM [3], [4]. Fig. 1 compares the CP-, KSP-, and UW-based OFDM transmit data structures.

(a) Data structure using CPs

(b) Data structure using KSP
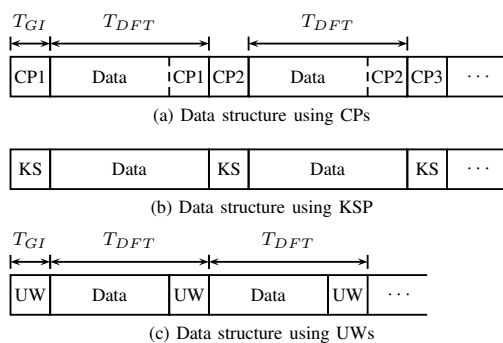
(c) Data structure using UWs

Figure 1: Transmit data structure using CPs, KSs or UWs.

In CP- as well as in UW-OFDM the linear convolution of the transmit signal with the channel impulse response is transformed into a cyclic convolution. However, there are some fundamental differences between the CP-based and the UW-based approach:

- Different to the CP, the UW is part of the DFT (discrete Fourier transform)-interval as indicated in Fig. 1.
- The CP is a random sequence, whereas the UW is deterministic. Thus, the UW can optimally be designed for particular needs like synchronization and/or channel estimation purposes at the receiver side.

The broadly known KSP-OFDM uses a structure similar to UW-OFDM, since the known symbol (KS) sequence is deterministic as well. The most important difference between KSP- and UW-OFDM is the fact, that the UW is part of the DFT interval, whereas the KS is not. On the one hand this characteristic of the UW implies the cyclic convolution property addressed above, and on the other hand, but no less importantly, the insertion of the UW within the DFT-interval introduces correlations in the frequency domain, which can advantageously be exploited by the receiver to improve the BER (bit error ratio) performance. Whilst in both schemes the deterministic sequences can be used for synchronization and channel estimation purposes, KSP-OFDM does not feature these correlations. We notice that KSP-OFDM coincides with ZP-OFDM (zero padded OFDM), if the KS sequence is set to zero.

In our concept described in [1] we suggested to generate UW-OFDM symbols by appropriately loading so-called redundant subcarriers. The minimization of the energy contribution of the redundant subcarriers turned out to be a challenge. We solved the problem by generating a zero UW in a first step, and by adding the desired UW in a separate second step. We showed that this approach generates OFDM symbols with much less redundant energy [2] than a single step or direct UW generation approach as e.g. described in [5]. Additionally, we optimized the positions of the redundant subcarriers to further reduce their energy contribution. We notice, that the concept in [5] generates completely different OFDM symbols compared to our approach in [1], and it has to deal with extremely high symbol energies and with the fact, that the performance depends on the particular shape of the UW. This is clearly in contrast to our approach, where the BER performance is independent of the particular shape of the UW due to the two-step generation approach. The BER behavior only depends on the freely selectable UW energy.

In this paper, we extend our results in [1], [2] by investigating several different linear data estimation concepts by applying methods from classical and Bayesian estimation theory. The paper is organized as follows: In Sec. 2 we briefly review the procedure of the unique word generation. The system model and some useful preparatory steps for the data estimation will be detailed in Sec. 3. Next we derive data estimators for UW-OFDM using classical estimation theory approaches in Sec. 4 which leads to ZF (zero forcing) equalizer concepts. Then, in Sec. 5 the linear Bayesian MMSE estimator is regarded. Finally, in Sec. 6 we highlight the BER performance of the introduced methods in the AWGN (additive white Gaussian noise) channel and in frequency selective indoor multipath environments. We conclude our work in Sec. 7.

Notation: Lower-case bold face variables $(\mathbf{a}, \mathbf{b}, \dots)$ indicate vectors, and upper-case bold face variables $(\mathbf{A}, \mathbf{B}, \dots)$ indicate matrices. To distinguish between time and frequency domain variables, we use a tilde to express frequency domain vectors and matrices $(\tilde{\mathbf{a}}, \tilde{\mathbf{A}}, \dots)$, respectively. We further use $\mathbb{C}$ to denote the set of complex numbers, $\mathbf{I}$ to denote the identity matrix, $(\cdot)^T$ to denote transposition, $(\cdot)^H$ to denote conjugate transposition, $E[\cdot]$ to denote expectation, and $\mathrm{tr}(\cdot)$ to denote the trace operator. For all signals and

systems the usual equivalent complex baseband representation is applied.

2. REVIEW OF UW-OFDM: UNIQUE WORD GENERATION

We briefly review our approach of introducing unique words in OFDM time domain symbols, for further details see [1], [2]. Let $\mathbf{x}_u \in \mathbb{C}^{N_u \times 1}$ be a predefined sequence which we call unique word. This unique word shall form the tail of each OFDM time domain symbol vector $\mathbf{x} = \begin{bmatrix} \mathbf{x}_d^T & \mathbf{x}_u^T \end{bmatrix}^T \in \mathbb{C}^{N \times 1}$, where only $\mathbf{x}_d \in \mathbb{C}^{(N-N_u) \times 1}$ is random and affected by the data. In the concept suggested in [1], [2] we generate an OFDM symbol $\mathbf{x} = \begin{bmatrix} \mathbf{x}_d^T & \mathbf{0}^T \end{bmatrix}^T$ with a zero UW in a first step, and we determine the final transmit symbol $\mathbf{x}' = \mathbf{x} + \begin{bmatrix} \mathbf{0}^T & \mathbf{x}_u^T \end{bmatrix}^T$ by adding the desired UW in time domain in a second step. As in conventional OFDM, the QAM data symbols (denoted by the vector $\tilde{\mathbf{d}} \in \mathbb{C}^{N_d \times 1}$) and the zero subcarriers (at the band edges and at DC) are specified in frequency domain as part of the vector $\tilde{\mathbf{x}}$, but here in addition the zero-word is specified in time domain as part of the vector $\mathbf{x} = \mathbf{F}_N^{-1} \tilde{\mathbf{x}}$. Here, $\mathbf{F}_N$ denotes the length-N DFT matrix with elements $[\mathbf{F}_N]_{kl} = e^{-j\frac{2\pi}{N}kl}$ for $k, l = 0, 1, ..., N-1$. The system of equations $\mathbf{x} = \mathbf{F}_N^{-1} \tilde{\mathbf{x}}$ with the introduced features can be fulfilled by spending some data subcarriers and instead introducing a set of redundant subcarriers. We let the redundant subcarrier symbols form the vector $\tilde{\mathbf{r}} \in \mathbb{C}^{N_r \times 1}$ with $N_r = N_u$, we further introduce a permutation matrix $\mathbf{P} \in \mathbb{C}^{(N_d+N_r) \times (N_d+N_r)}$, and form an OFDM symbol (containing $N - N_d - N_r$ zero subcarriers) in frequency domain by $\tilde{\mathbf{x}} = \mathbf{BP} \begin{bmatrix} \tilde{\mathbf{d}} \\ \tilde{\mathbf{r}} \end{bmatrix}$. Here, $\mathbf{B} \in \mathbb{C}^{N \times (N_d+N_r)}$ models the insertion of the zero subcarrier symbols. We will detail the reason for the introduction of the permutation matrix $\mathbf{P}$ and its specific construction shortly below. The time–frequency relation $\mathbf{F}_N^{-1} \tilde{\mathbf{x}} = \mathbf{x}$ can now be written as

$$\mathbf{F}_N^{-1} \mathbf{BP} \begin{bmatrix} \tilde{\mathbf{d}} \\ \tilde{\mathbf{r}} \end{bmatrix} = \begin{bmatrix} \mathbf{x}_d \\ \mathbf{0} \end{bmatrix}. \tag{1}$$

With $\mathbf{M} = \mathbf{F}_N^{-1} \mathbf{BP} = \begin{bmatrix} \mathbf{M}_{11} & \mathbf{M}_{12} \\ \mathbf{M}_{21} & \mathbf{M}_{22} \end{bmatrix}$, where $\mathbf{M}_{kl}$ are appropriate sized sub-matrices, it follows that $\mathbf{M}_{21} \tilde{\mathbf{d}} + \mathbf{M}_{22} \tilde{\mathbf{r}} = \mathbf{0}$, and hence $\tilde{\mathbf{r}} = -\mathbf{M}_{22}^{-1} \mathbf{M}_{21} \tilde{\mathbf{d}}$. With the matrix $\mathbf{T} = -\mathbf{M}_{22}^{-1} \mathbf{M}_{21} \in \mathbb{C}^{N_r \times N_d}$, the vector of redundant subcarrier symbols can thus be determined by the linear mapping $\tilde{\mathbf{r}} = \mathbf{T} \tilde{\mathbf{d}}$. The construction of $\mathbf{T}$ and thus also the energy of the redundant subcarrier symbols highly depend on the choice of $\mathbf{P}$. In [1] we suggested to choose $\mathbf{P}$ by a minimization of the symbol energy $E_{\mathbf{x}'}$ which leads to the optimization problem $\mathbf{P} = \arg\min \{\mathrm{tr}(\mathbf{TT}^H)\}$. In Sec. 6 we give an example of the optimum redundant subcarrier distribution for a specific parameter setup.

In the following, we use the notation $\tilde{\mathbf{c}}$ with

$$\tilde{\mathbf{c}} = \mathbf{P} \begin{bmatrix} \tilde{\mathbf{d}} \\ \tilde{\mathbf{r}} \end{bmatrix} = \mathbf{P} \begin{bmatrix} \mathbf{I} \\ \mathbf{T} \end{bmatrix} \tilde{\mathbf{d}} = \mathbf{G} \tilde{\mathbf{d}}, \tag{2}$$

where the matrix $\mathbf{G} = \mathbf{P} \begin{bmatrix} \mathbf{I} & \mathbf{T}^T \end{bmatrix}^T \in \mathbb{C}^{(N_d+N_r) \times N_d}$ can be interpreted as a code generator matrix for a systematic complex valued Reed Solomon code, that generates the code words $\tilde{\mathbf{c}}$. With (2) and the frequency domain version of the UW $\tilde{\mathbf{x}}_u = \mathbf{F}_N \begin{bmatrix} \mathbf{0} & \mathbf{x}_u \end{bmatrix}^T$, the transmit symbol can now be written as $\mathbf{x}' = \mathbf{F}_N^{-1}(\mathbf{BG} \tilde{\mathbf{d}} + \tilde{\mathbf{x}}_u)$.

3. SYSTEM MODEL AND PREPARATORY STEPS

After the transmission over a dispersive (e.g. multipath) channel, applying a DFT and discarding the zero subcarriers, the received OFDM frequency domain symbol $\tilde{\mathbf{y}}_d \in \mathbb{C}^{(N_d+N_r) \times 1}$ can be modeled as

$$\tilde{\mathbf{y}}_d = \mathbf{B}^T \mathbf{F}_N \mathbf{H}_c \mathbf{F}_N^{-1}(\mathbf{BG}\tilde{\mathbf{d}} + \tilde{\mathbf{x}}_u) + \mathbf{B}^T \mathbf{F}_N \mathbf{n}, \tag{3}$$

where $\mathbf{n} \in \mathbb{C}^{N \times 1}$ represents a zero-mean Gaussian (time domain) noise vector with the covariance matrix $\sigma_n^2 \mathbf{I}$, and $\mathbf{H}_c \in \mathbb{C}^{N \times N}$ denotes a cyclic convolution matrix originating from the zero-padded vector of channel impulse response coefficients $\mathbf{h}_c \in \mathbb{C}^{N \times 1}$. With the downsized diagonal matrix $\widetilde{\mathbf{H}}_d = \mathbf{B}^T \mathbf{F}_N \mathbf{H}_c \mathbf{F}_N^{-1} \mathbf{B}$ ($\widetilde{\mathbf{H}}_d \in \mathbb{C}^{(N_d+N_r) \times (N_d+N_r)}$) containing the channel frequency response samples corresponding to the data and redundant subcarrier positions, the received symbol can now be written in the form of the *affine* model

$$\tilde{\mathbf{y}}_d = \widetilde{\mathbf{H}}_d \mathbf{G} \tilde{\mathbf{d}} + \widetilde{\mathbf{H}}_d \mathbf{B}^T \tilde{\mathbf{x}}_u + \mathbf{B}^T \mathbf{F}_N \mathbf{n}. \tag{4}$$

Note that (assuming that the channel matrix $\widetilde{\mathbf{H}}_d$ or at least an estimate of it is available) $\widetilde{\mathbf{H}}_d \mathbf{B}^T \tilde{\mathbf{x}}_u$ represents the known portion contained in the received vector $\tilde{\mathbf{y}}_d$ originating from the UW. As a first preparatory step we therefore subtract the UW influence to obtain the corrected symbol in the form of the *linear* model

$$\begin{aligned} \tilde{\mathbf{y}} &= \tilde{\mathbf{y}}_d - \widetilde{\mathbf{H}}_d \mathbf{B}^T \tilde{\mathbf{x}}_u \tag{5} \\ &= \widetilde{\mathbf{H}}_d \mathbf{G} \tilde{\mathbf{d}} + \tilde{\mathbf{v}}, \tag{6} \end{aligned}$$

with the noise vector $\tilde{\mathbf{v}} = \mathbf{B}^T \mathbf{F}_N \mathbf{n}$.

4. CLASSICAL DATA ESTIMATORS – ZERO FORCING SOLUTIONS

In this section we consider classical unbiased data estimators of the form

$$\widehat{\tilde{\mathbf{d}}} = \mathbf{E} \tilde{\mathbf{y}}, \tag{7}$$

where $\mathbf{E} \in \mathbb{C}^{N_d \times (N_d+N_r)}$ describes the equalizer. Note that in classical estimation the data vector is assumed to be deterministic but unknown. In order for the estimator to be unbiased we require

$$\begin{aligned} E[\widehat{\tilde{\mathbf{d}}}] &= E[\mathbf{E}\tilde{\mathbf{y}}] \\ &= \mathbf{E}E[\widetilde{\mathbf{H}}_d \mathbf{G} \tilde{\mathbf{d}} + \tilde{\mathbf{v}}] \\ &= \mathbf{E}\widetilde{\mathbf{H}}_d \mathbf{G} \tilde{\mathbf{d}} \\ &= \tilde{\mathbf{d}}. \end{aligned}$$

Consequently, the unbiased constraint takes on the form

$$\mathbf{E}\widetilde{\mathbf{H}}_d \mathbf{G} = \mathbf{I}, \tag{8}$$

which is equivalent to the ZF criterion for linear equalizers. The solution to (8) is ambiguous. To show this we consider a singular value decomposition of $\widetilde{\mathbf{H}}_d \mathbf{G}$ as

$$\widetilde{\mathbf{H}}_d \mathbf{G} = \mathbf{U} \begin{bmatrix} \mathbf{\Sigma} \\ \mathbf{0} \end{bmatrix} \mathbf{V}^H, \tag{9}$$

with unitary matrices $\mathbf{U}$ and $\mathbf{V}$, and with the diagonal matrix $\mathbf{\Sigma}$ having as its main diagonal the singular values of $\widetilde{\mathbf{H}}_d \mathbf{G}$. With (9) the unbiased constraint (or ZF criterion) (8) can be re-written as

$$\mathbf{E}\mathbf{U} \begin{bmatrix} \mathbf{\Sigma} \\ \mathbf{0} \end{bmatrix} \mathbf{V}^H = \mathbf{I}. \tag{10}$$

It is easy to see that (10) and therefore also (8) is fulfilled by every equalizer of the form

$$\mathbf{E} = \mathbf{V} \begin{bmatrix} \mathbf{\Sigma}^{-1} & \mathbf{A} \end{bmatrix} \mathbf{U}^H \tag{11}$$

with arbitrary $\mathbf{A}$.

Since the solution to the unbiased constraint is not unambiguous it makes sense to look for the optimum solution which is commonly known as the best linear unbiased estimator.

4.1 Best Linear Unbiased Estimator (BLUE)

By applying the Gauss-Markov theorem [6] to (6) the BLUE and consequently the optimum ZF equalizer ($\mathbf{E}_{\text{BLUE}} = \mathbf{E}_{\text{ZF,opt}}$) follows to

$$\mathbf{E}_{\text{BLUE}} = (\mathbf{G}^H \widetilde{\mathbf{H}}_d^H \mathbf{C}_{\tilde{v}\tilde{v}}^{-1} \widetilde{\mathbf{H}}_d \mathbf{G})^{-1} \mathbf{G}^H \widetilde{\mathbf{H}}_d^H \mathbf{C}_{\tilde{v}\tilde{v}}^{-1}. \tag{12}$$

We note that since the noise in (6) is assumed to be Gaussian, (12) is also the MVU (minimum variance unbiased) estimator. With the noise covariance matrix $\mathbf{C}_{\tilde{v}\tilde{v}} = E\left[\tilde{\mathbf{v}}\tilde{\mathbf{v}}^H\right] = N\sigma_n^2 \mathbf{I}$ we immediately obtain

$$\mathbf{E}_{\text{BLUE}} = (\mathbf{G}^H \widetilde{\mathbf{H}}_d^H \widetilde{\mathbf{H}}_d \mathbf{G})^{-1} \mathbf{G}^H \widetilde{\mathbf{H}}_d^H. \tag{13}$$

The covariance matrix of $\hat{\tilde{\mathbf{d}}} = \mathbf{E}_{\text{BLUE}}\tilde{\mathbf{y}}$, or equivalently the covariance matrix of the error $\tilde{\mathbf{e}} = \tilde{\mathbf{d}} - \hat{\tilde{\mathbf{d}}}$ is given by

$$\mathbf{C}_{\tilde{e}\tilde{e}} = N\sigma_n^2 (\mathbf{G}^H \widetilde{\mathbf{H}}_d^H \widetilde{\mathbf{H}}_d \mathbf{G})^{-1}, \tag{14}$$

cf. [6].

To conclude this section we will depict the interrelationship between $\mathbf{E}_{\text{BLUE}}$ and the solution in (11). $\mathbf{E}_{\text{BLUE}}$ as given in (13) represents nothing but the Moore-Penrose pseudoinverse of $\widetilde{\mathbf{H}}_d \mathbf{G}$. By using the singular value decomposition as in (9), (13) can be re-written as

$$\begin{aligned}
\mathbf{E}_{\text{BLUE}} &= (\mathbf{V} \begin{bmatrix} \mathbf{\Sigma}^H & \mathbf{0} \end{bmatrix} \mathbf{U}^H \mathbf{U} \begin{bmatrix} \mathbf{\Sigma} \\ \mathbf{0} \end{bmatrix} \mathbf{V}^H)^{-1} \mathbf{V} \begin{bmatrix} \mathbf{\Sigma}^H & \mathbf{0} \end{bmatrix} \mathbf{U}^H \\
&= (\mathbf{V}\mathbf{\Sigma}^H \mathbf{\Sigma} \mathbf{V}^H)^{-1} \mathbf{V} \begin{bmatrix} \mathbf{\Sigma}^H & \mathbf{0} \end{bmatrix} \mathbf{U}^H \\
&= \mathbf{V}(\mathbf{\Sigma}^H \mathbf{\Sigma})^{-1} \mathbf{V}^H \mathbf{V} \begin{bmatrix} \mathbf{\Sigma}^H & \mathbf{0} \end{bmatrix} \mathbf{U}^H \\
&= \mathbf{V} \begin{bmatrix} (\mathbf{\Sigma}^H \mathbf{\Sigma})^{-1} \mathbf{\Sigma}^H & \mathbf{0} \end{bmatrix} \mathbf{U}^H \\
&= \mathbf{V} \begin{bmatrix} \mathbf{\Sigma}^{-1} & \mathbf{0} \end{bmatrix} \mathbf{U}^H.
\end{aligned} \tag{15}$$

By comparing this result with (11) it can be concluded that $\mathbf{E}_{\text{BLUE}}$ corresponds to the solution in (11) for the particular case $\mathbf{A} = \mathbf{0}$.

4.2 Sub-Optimum ZF Receiver Structures

Any unbiased linear data estimator, or equivalently, any linear zero forcing equalizer has to fulfill (8). As already shown above the ZF solution is ambiguous for the UW-OFDM transmission model described in (6). Another quite intuitive and straight forward ZF solution is given by

$$\mathbf{E}_{\text{CI}} = \begin{bmatrix} \mathbf{I} & \mathbf{0} \end{bmatrix} \mathbf{P}^T \widetilde{\mathbf{H}}_d^{-1} = \widetilde{\mathbf{H}}_{d,1}^{-1} \begin{bmatrix} \mathbf{I} & \mathbf{0} \end{bmatrix} \mathbf{P}^T. \tag{16}$$

This equalizer extracts at first the data subcarriers and then inverts the channel on these subcarriers. Here, $\widetilde{\mathbf{H}}_{d,1}$ is a matrix that contains on its main diagonal the channel frequency response samples corresponding to the data subcarriers. Clearly this procedure fulfills (8). In the following we will refer to this equalizer as the channel inversion (CI) receiver. The channel inversion receiver represents a low complex solution since $\widetilde{\mathbf{H}}_{d,1}$ has a diagonal structure, but it does not take advantage of the correlations introduced by $\mathbf{G}$ at the transmitter side. The covariance matrix of $\hat{\tilde{\mathbf{d}}} = \mathbf{E}_{\text{CI}}\tilde{\mathbf{y}}$, or equivalently the covariance matrix of the error $\tilde{\mathbf{e}} = \tilde{\mathbf{d}} - \hat{\tilde{\mathbf{d}}}$ can easily shown to be

$$\mathbf{C}_{\tilde{e}\tilde{e}} = N\sigma_n^2 \mathbf{E}_{\text{CI}} \mathbf{E}_{\text{CI}}^H = N\sigma_n^2 (\widetilde{\mathbf{H}}_{d,1}^H \widetilde{\mathbf{H}}_{d,1})^{-1}. \tag{17}$$

Next we address another quite intuitive equalizer that exploits a-priori knowledge, namely, that the samples within the guard interval of an OFDM symbol must be zero after the channel inversion in the noiseless case (given that the influence of $\tilde{\mathbf{x}}_u$ has already been subtracted as indicated in (5)). In the presence of noise we therefore simply force the guard interval samples to zero which is achieved by an equalizer of the form

$$\mathbf{E}_{\text{TDW}} = \begin{bmatrix} \mathbf{I} & \mathbf{0} \end{bmatrix} \mathbf{P}^T \mathbf{B}^T \mathbf{F}_N \mathbf{\Theta} \mathbf{F}_N^{-1} \mathbf{B} \widetilde{\mathbf{H}}_d^{-1}, \tag{18}$$

where $\mathbf{\Theta} = \begin{bmatrix} \mathbf{I} & \mathbf{0} \\ \mathbf{0} & \mathbf{0} \end{bmatrix}$. The time domain windowing (TDW) equalizer starts with an inversion of the channel, next the zero subcarrier symbols are added again in order to be able to transform back to time domain with a length-N IDFT. Here a windowing (described by $\mathbf{\Theta}$) takes place, where the guard interval samples are forced to zero. Next a transformation back to frequency domain is performed, the zero subcarriers are excluded again, a re-sorting is done, and finally the data symbols are extracted. It can easily be shown, that $\mathbf{E}_{\text{TDW}}$ also fulfills (8). The covariance matrix of $\hat{\tilde{\mathbf{d}}} = \mathbf{E}_{\text{TDW}}\tilde{\mathbf{y}}$, or equivalently the covariance matrix of the error $\tilde{\mathbf{e}} = \tilde{\mathbf{d}} - \hat{\tilde{\mathbf{d}}}$ is given by

$$\mathbf{C}_{\tilde{e}\tilde{e}} = N\sigma_n^2 \mathbf{E}_{\text{TDW}} \mathbf{E}_{\text{TDW}}^H. \tag{19}$$

5. LINEAR BAYESIAN DATA ESTIMATOR – LMMSE SOLUTION

We now turn to the widely used linear minimum mean square error data estimator which is derived with the help of the Bayesian approach. In the Bayesian approach the data vector is assumed to be the realization of a random vector instead of a deterministic and unknown vector as in the classical estimation theory applied above. By applying the Bayesian Gauss-Markov theorem [6] to (6), where we now assume $\tilde{\mathbf{d}}$ to be the realization of a random vector, and assuming that $\mathbf{C}_{\tilde{d}\tilde{d}} = \sigma_d^2 \mathbf{I}$ and $\mathbf{C}_{\tilde{v}\tilde{v}} = \sigma_v^2 \mathbf{I} = N\sigma_n^2 \mathbf{I}$, the LMMSE equalizer follows to

$$\mathbf{E}_{\text{LMMSE}} = \mathbf{G}^H \left(\mathbf{G}\mathbf{G}^H + \frac{N\sigma_n^2}{\sigma_d^2} (\widetilde{\mathbf{H}}_d^H \widetilde{\mathbf{H}}_d)^{-1} \right)^{-1} \widetilde{\mathbf{H}}_d^{-1}. \tag{20}$$

With the introduction of the Wiener smoothing matrix

$$\mathbf{W} = \mathbf{G}^H \left(\mathbf{G}\mathbf{G}^H + \frac{N\sigma_n^2}{\sigma_d^2} (\widetilde{\mathbf{H}}_d^H \widetilde{\mathbf{H}}_d)^{-1} \right)^{-1}, \tag{21}$$

the LMMSE equalizer can be written as $\mathbf{E}_{\text{LMMSE}} = \mathbf{W} \widetilde{\mathbf{H}}_d^{-1}$, which allows the following interpretation of its mode of operation: The LMMSE equalizer acts as a composition of a simple channel inversion stage (multiplication with $\widetilde{\mathbf{H}}_d^{-1}$ as in (16)) and a Wiener smoothing operation (multiplication with $\mathbf{W}$). The Wiener smoothing operation exploits the correlations between subcarrier symbols which have been introduced by the redundant subcarriers at the transmitter, and acts as a noise reduction operation on the subcarriers. By applying the matrix inversion lemma, it can easily be shown that the equalizer can equivalently be determined by

$$\mathbf{E}_{\text{LMMSE}} = (\mathbf{G}^H \widetilde{\mathbf{H}}_d^H \widetilde{\mathbf{H}}_d \mathbf{G} + \frac{N\sigma_n^2}{\sigma_d^2} \mathbf{I})^{-1} \mathbf{G}^H \widetilde{\mathbf{H}}_d^H. \tag{22}$$

Expression (22) shows strong similarities to the optimum linear ZF equalizer in (13). For $\sigma_n^2 = 0$ the LMMSE equalizer coincides with the optimum linear ZF equalizer. The expression for $\mathbf{C}_{\tilde{e}\tilde{e}}$ can be shown to be

$$\mathbf{C}_{\tilde{e}\tilde{e}} = N\sigma_n^2 (\mathbf{G}^H \widetilde{\mathbf{H}}_d^H \widetilde{\mathbf{H}}_d \mathbf{G} + \frac{N\sigma_n^2}{\sigma_d^2} \mathbf{I})^{-1}. \tag{23}$$

6. SIMULATION RESULTS

Fig. 2 shows the block diagram of the simulated UW-OFDM system. The transmitter processing starts with (outer) channel coding, interleaving and QAM-mapping. We used the same outer convolutional encoder with the industry standard rate 1/2, constraint length 7 code with generator polynomials (133, 171) as defined in [7]. Next, the redundant subcarrier symbols are determined. After assembling the OFDM symbol in frequency domain, which is composed of $\tilde{\mathbf{d}}$, $\tilde{\mathbf{r}}$, and a set of zero subcarriers, the IFFT is computed.

Finally, the UW is added in time domain. At the receiver side the processing for one OFDM symbol starts with an FFT, then the influence of the UW is subtracted. Next the linear data estimation is applied by using one of the introduced data estimation methods, where we assumed perfect channel knowledge at the receiver. Finally demapping, deinterleaving and decoding are performed. A soft decision Viterbi algorithm is applied for decoding. The main diagonal of matrix $\mathbf{C}_{\tilde{e}\tilde{e}}$ is used to specify the varying noise variances along the data symbols after data estimation.
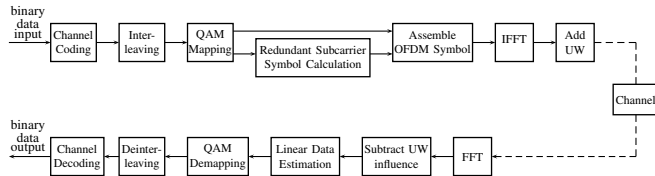
Figure 2: Block diagram for simulation analysis.

In [1] we compared our UW-OFDM approach with the CP-OFDM based IEEE 802.11a WLAN standard [7] and showed that UW-OFDM outperforms CP-OFDM in frequency selective indoor environments. Also in this work we use the same parameter setup which is adapted to the 802.11a standard wherever possible: $N = 64$, sampling frequency $f_s = 20$MHz, DFT period $T_{DFT} = 3.2\mu s$, guard duration $T_{GI} = 800$ns, QPSK as modulation scheme, subcarrier spacing $\Delta f = 315.2$ kHz, $N_r = N_u = 16$, $N_d = 36$. As in [7] the indices of the zero subcarriers within an OFDM symbol $\tilde{\mathbf{x}}$ are set to $\{0, 27, 28,...,37\}$. The indices of the redundant subcarriers are chosen to be $\{2, 6, 10, 14, 17, 21, 24, 26, 38, 40, 43, 47, 50, 54, 58, 62\}$. This set (which can also be expressed by an appropriate permutation matrix $\mathbf{P}$) minimizes the energy of the redundant subcarriers on average and has been obtained by a heuristic optimization approach [8]. Since we focus on data estimation procedures in this work rather than on synchronization or channel estimation approaches we chose the zero UW for the BER simulations below.

6.1 Simulation Results in the AWGN Channel

Clearly, OFDM is designed for data transmission in frequency selective environments. Nevertheless, we start our comparison with simulation results in the AWGN channel, since these results provide first interesting insights. In Fig. 3 the BER performance of the different data estimators is compared under AWGN conditions. As in all following BER figures we present curves for the case when no outer code is used (we label it 'uncoded' case in the figures), and for an outer coding rate $r = \frac{1}{2}$.
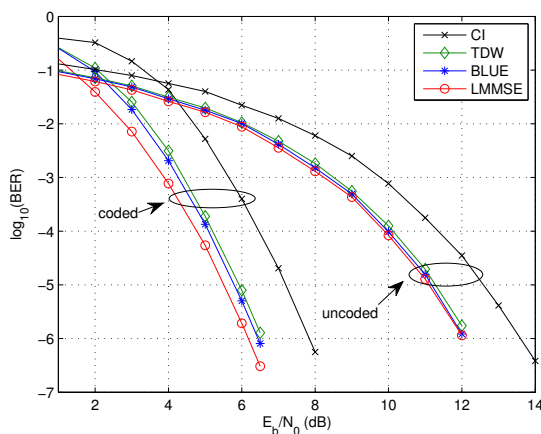

Figure 3: BER performance of the data estimators in the AWGN channel.

We start the discussion with the uncoded case: As expected the CI estimator shows the worst performance, since it completely ignores the information present on the redundant subcarriers. Surprisingly, the very simple and intuitive TDW data estimator performs almost as well as the BLUE and the LMMSE in the AWGN environment. At a BER of 10^{-6} these three estimators which all make use of the a-priori knowledge introduced by the zero UW outperform the CI estimator by around 1.5dB. The trend is similar for $r = \frac{1}{2}$.

6.2 Simulation Results in Frequency Selective Indoor Environments

For the simulation of indoor multipath channels we applied the model described in [9], which has also been used during the IEEE 802.11a standardization process. The channel impulse responses are modeled as tapped delay lines, each tap with uniformly distributed phase and Rayleigh distributed magnitude, and with power decaying exponentially. For illustration purposes we use two different channel snapshots in this section, each channel featuring a delay spread of 100 ns, and a total duration not exceeding the guard interval. The frequency responses are shown in Fig. 4. Channel A
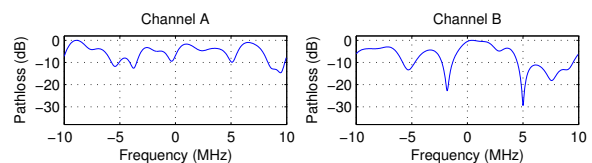

Figure 4: Frequency responses of multipath channel snapshots.

does not show any deep fading holes, whereas channel B features two spectral notches within the system bandwidth, one at a data subcarrier position, the other one at a redundant subcarrier position.

Let us first interpret the results for channel A, cf. Fig. 5. We observe similar trends as in the AWGN case, but now the LMMSE estimator and the BLUE clearly outperform the TDW estimator. For uncoded transmission the TDW outperforms the CI estimator by 1.9dB (again at a BER of 10^{-6}), the BLUE and the LMMSE estimator gain 2.8dB and 2.9dB, respectively. For $r = \frac{1}{2}$ the corresponding gains shrink to 1.1dB, 1.5dB and 1.7dB, respectively.

Finally Fig. 6 shows the simulation results for channel B with its deep spectral notches. The bad performance of the CI and the TDW estimators in the uncoded transmission is very noticeable. Here the performance gain of the BLUE and the LMMSE estimator is significant. The performance of the CI estimator is dominated by the weak BER behavior of data subcarrier symbols corresponding to deep spectral notches in the channel frequency response, while the LMMSE estimator (and similarly the BLUE) considerably decrease the noise on that subcarriers. (They decrease the noise variance on all subcarriers, but the effect is impressive on subcarriers corresponding to deep spectral notches, cf. [1]). In coded transmission the performance loss of the CI estimator compared to the best performing LMMSE estimator decreases to 1.4dB. The significant improvement of the CI estimator in the coded case was expected as this corresponds to the usual coding gain as it is also observed in CP-OFDM. Somewhat unexpected, and in contrast to the uncoded results and those in an AWGN channel and in channel A, the TDW equalizer performs almost 0.9dB worse compared to the CI equalizer at a BER of 10^{-6}. To understand this effect we will now have a closer look on the way the TDW estimator works. In fact, although it is hardly noticeable in Fig. 6, in the uncoded case the TDW only outperforms the CI estimator in the high E_b/N_0 range, but performs worse in the low E_b/N_0 range (0–15 dB). However, this is the interesting E_b/N_0 range for coded transmission. We will now have a look on the noise variances (after equalization) and later on the BERs on the individual data subcarriers.

Fig. 7a and 7b show the normalized noise variances after equalization at a fixed E_b/N_0 ($E_b/N_0 = 4$ dB) for both data estimators. We observe that on the data subcarrier with index 11 the noise vari-
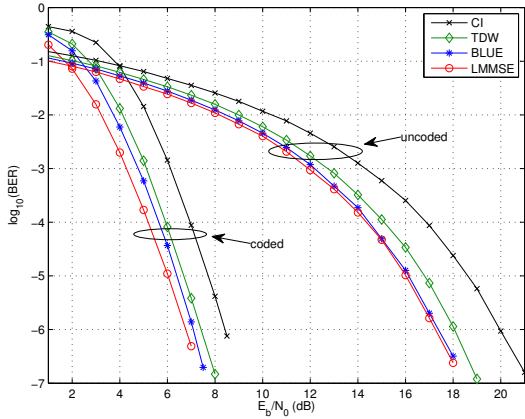
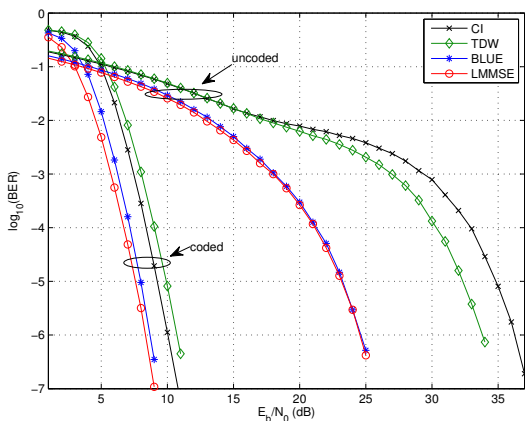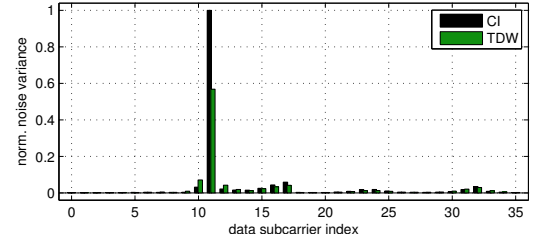Figure 5: BER performance of the data estimators for channel A.

Figure 6: BER performance of the data estimators for channel B.

(a) Noise variances, total view

(b) Noise variances, zoomed in

Figure 7: Subchannel noise variances after CI and TDW data estimation, and difference $BER_{TDW} - BER_{CI}$ per subcarrier.
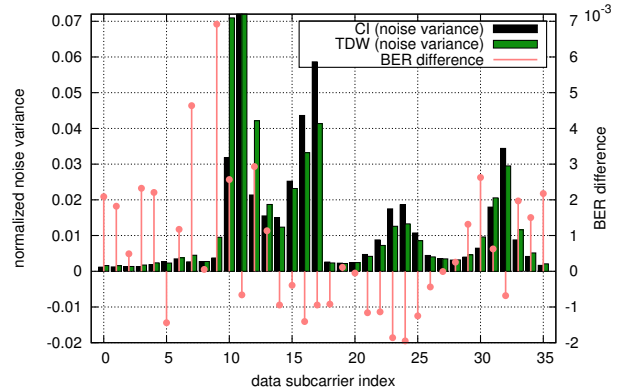
ance is tremendously reduced by the TDW compared to the CI estimator. This data subcarrier corresponds to the deep spectral notch around 5 MHz in the channel's frequency response. However, we also notice that the noise variances on data subcarriers around data symbol No. 11 are a little bit higher for the TDW compared to the CI estimator. On average (when averaged over all data subcarriers) the TDW equalizer clearly reduces the noise power compared to the CI equalizer, but besides a significant noise reduction on highly attenuated subcarriers, the TDW equalizer 'distributes' some noise onto neighboring subcarriers. Fig. 7b additionally shows the difference between the resulting BERs of the TDW and the CI estimators on a subcarrier basis. We observe, that the tremendous noise reduction by the TDW equalizer on the 11th data subcarrier indeed leads to a lower subcarrier BER compared to the CI equalizer, but the improvement is minor. In return, the higher noise variances on the adjacent data subcarriers lead to increased corresponding subcarrier BERs for the TDW estimator. In total the increase of these subcarrier BERs lead to a worse overall BER performance of the TDW compared to the CI estimator for these E_b/N_0 values. The overall noise reduction by the TDW estimator is not translated to an overall BER gain for that particular channel for these E_b/N_0 values.

7. CONCLUSION

In this work we investigated several linear data estimators specifically designed for UW-OFDM. We introduced data estimators following the principles of classical estimation theory which lead to ZF equalizers. Two simple and intuitive ZF equalizers and the optimum ZF equalizer corresponding to the BLUE have been discussed. Following the Bayesian estimation principle the LMMSE estimator has been presented. We demonstrated the bit error behavior of the proposed estimators in the AWGN channel and in frequency selec-

tive indoor environments. In frequency selective channels featuring deep fading holes, the BLUE and, especially, the LMMSE estimator significantly outperform the simple ZF estimators.

REFERENCES

[1] M. Huemer, C. Hofbauer, J.B. Huber, "The Potential of Unique Words in OFDM", in the *Proceedings of the 15th International OFDM-Workshop*, Hamburg, Germany, pp. 140-144, September 2010.

[2] A. Onic, M. Huemer, "Direct versus Two-Step Approach for Unique Word Generation in UW-OFDM", in the *Proceedings of the 15th International OFDM-Workshop*, Hamburg, Germany, pp.145-149, September 2010.

[3] S. Tang, F. Yang, K. Peng, C. Pan, K. Gong, Z. Yang, "Iterative channel estimation for block transmission with known symbol padding - a new look at TDS-OFDM", in the *Proceedings of the IEEE Global Telecommunications Conference 2007 (GLOBECOM 2007)*, pp. 4269-4273, Nov. 2007.

[4] D. Van Welden, H. Steendam, M. Moeneclaey, "Iterative DA/DD channel estimation for KSP-OFDM", in the *Proceedings IEEE International Conference on Communications 2008 (ICC 2008)*, pp. 693-697, May 2008.

[5] R. Cendrillon, M. Moonen, "Efficient equalizers for single and multi-carrier environments with known symbol padding", in the *Proceedings of the IEEE International Symposium on Signal Processing and its Applications 2001 (ISSPA 2001)*, August 2001, Pages 607-610.

[6] S. Kay, *Fundamentals of Statistical Signal Processing: Estimation Theory*, Prentice Hall, Rhode Island 1993.

[7] IEEE Std 802.11a-1999, Part 11: Wireless LAN Medium Access Control (MAC) and Physical Layer (PHY) specifications: High-Speed Physical Layer in the 5 GHz Band, 1999.

[8] Z. Michalewicz, D.B. Fogel, *How to Solve It: Modern Heuristics*, Springer, Berlin, Germany, 2nd Ed., 2004.

[9] J. Fakatselis, Criteria for 2.4 GHz PHY Comparison of Modulation Methods. Document IEEE 1997; P802.11-97/157r1.